

Microscopic calculations of transport properties of neutron matter

Omar Benhar^{1,2}, Artur Polls³, Marco Valli^{1,2}, and Isaac Vidaña⁴

¹ *INFN, Sezione di Roma. I-00185 Roma, Italy*

² *Dipartimento di Fisica,*

Università “La Sapienza”. I-00185 Roma, Italy

³ *Departament d'Estructura i Constituents de la Matèria. E-08028 Barcelona, Spain*

⁴ *Centro de Física Computacional,*

Department of Physics, University of Coimbra,

3004-516 Coimbra, Portugal

(Dated: November 5, 2018)

We discuss the results of calculations of the shear viscosity and thermal conductivity of pure neutron matter, carried out within the Landau-Abrikosov-Khalatnikov formalism. The probability of neutron-neutron collisions in the nuclear medium has been obtained from a realistic potential, using both the correlated basis function and the G -matrix approach. The results of our work indicate that medium modifications of nucleon-nucleon scattering are large, their inclusion leading to a dramatic enhancement of the transport coefficients. On the other hand, the results obtained from the two theoretical schemes appear to be in fairly good agreement.

PACS numbers: 24.10.Cn, 25.30.Fj, 61.12.Bt

I. INTRODUCTION

The knowledge of transport properties of neutron matter is relevant to the understanding of a variety of neutron star properties. Viscosity plays a crucial role in determining the onset of the gravitational-wave driven instability, associated with the excitation of r -modes, in rapidly rotating stars [1], while thermal conductivity is one of the factors determining neutron star cooling [2].

Unlike the equation of state (EOS), which is generally obtained from realistic dynamical models, strongly constrained from nuclear systematics and nucleon-nucleon scattering data, the non-equilibrium properties of neutron star matter are often studied using oversimplified models of the nucleon-nucleon (NN) interaction.

The main difficulty involved in the calculation of the transport coefficients within the formalism originally developed by Abrikosov and Khalatnikov [3], based on Landau theory of normal Fermi liquids [4], is the determination of the nucleon-nucleon (NN) collision probability in the nuclear medium. Most studies of the transport properties of neutron star matter have circumvented this problem neglecting medium modifications of the NN cross sections altogether, and using the measured NN scattering phase shifts to construct the collision probability [5, 6, 7].

Nuclear many body theory provides a consistent framework to obtain the in-medium NN cross section and the transport coefficients of nuclear matter from realistic NN potentials, using either the G -matrix [8] or the correlated basis function (CBF) [10] formalism. In both approaches one can define a well behaved effective interaction, suitable for use in standard perturbation theory in the Fermi gas basis and allowing for a *consistent* treatment of equilibrium and non-equilibrium properties [8, 9, 10].

In this paper we discuss the results of calculations of

the shear viscosity and thermal conductivity of pure neutron matter, carried out using the CBF and G -matrix effective interactions.

In Section II, after outlining the elements of nuclear many body theory, we analyze the main features of the CBF and G -matrix effective interactions, while Section III is devoted to the discussion of the in-medium NN cross section in the kinematical setup relevant to the calculation of the transport coefficients. The main features of the Abrikosov-Khalatnikov formalism are reviewed in Section IV, where we also present the results of numerical calculations. Finally, in Section V we summarize our findings and state the conclusions.

II. EFFECTIVE INTERACTIONS IN NUCLEAR MANY BODY THEORY

Nuclear many body theory (NMBT) is based on the tenet that nuclei can be described in terms of point like nucleons, whose dynamics are dictated by the hamiltonian

$$H = \sum_i \frac{\mathbf{k}_i^2}{2m} + \sum_{j>i} v_{ij} + \sum_{k>j>i} V_{ijk} , \quad (1)$$

\mathbf{k}_i and m being the momentum of the i -th nucleon and its mass, respectively.

The nucleon-nucleon (NN) potential v_{ij} reduces to the Yukawa one-pion exchange potential at large distances, while its behavior at short and intermediate range is determined by a fit of deuteron properties and NN scattering phase shifts. The state-of-the-art NN parametrization referred to as Argonne v_{18} potential [11] is written

in the form

$$v_{ij} = \sum_{n=1}^{18} v_n(r_{ij}) O_{ij}^n. \quad (2)$$

In the above equation

$$O_{ij}^{n \leq 6} = [1, (\boldsymbol{\sigma}_i \cdot \boldsymbol{\sigma}_j), S_{ij}] \otimes [1, (\boldsymbol{\tau}_i \cdot \boldsymbol{\tau}_j)] \quad (3)$$

where $\boldsymbol{\sigma}_i$ and $\boldsymbol{\tau}_i$ are Pauli matrices acting in spin and isospin space, respectively, and

$$S_{ij} = \frac{3}{r_{ij}^2} (\boldsymbol{\sigma}_i \cdot \mathbf{r}_{ij})(\boldsymbol{\sigma}_j \cdot \mathbf{r}_{ij}) - (\boldsymbol{\sigma}_i \cdot \boldsymbol{\sigma}_j). \quad (4)$$

The operators corresponding to $n = 7, \dots, 14$ are associated with the non-static components of the NN interaction, while those corresponding to $n = 15, \dots, 18$ account for small charge symmetry violations. Being fit to the full Nijmegen phase shifts data base, as well as to low energy scattering parameters and deuteron properties, the Argonne v_{18} potential provides an accurate description of the scattering data by construction.

The three-nucleon potential V_{ijk} , whose inclusion is needed to reproduce the observed binding energies of the three-nucleon system and the empirical nuclear matter equilibrium properties, consists of the Fujita-Miyazawa two-pion exchange potential supplemented by a purely phenomenological repulsive contribution [12].

The predictive power of the dynamical model based on the hamiltonian of Eq.(1) has been extensively tested by computing the energies of the ground and low-lying excited states of nuclei with $A \leq 12$. The results of these studies, in which the many body Schrödinger equation is solved *exactly* using stochastic methods, turn out to be in excellent agreement with experimental data [13]. Accurate calculations can also be carried out for uniform nuclear matter, exploiting translational invariance and using the stochastic method [14], the variational approach [15], or G -matrix perturbation theory [16, 17].

One of the most prominent features of the NN potential is the strongly repulsive core, whose cleanest manifestation is the observed saturation of nuclear charge densities. Due to the presence of the core, the NN potential cannot be used to carry out *ab initio* microscopic calculations of nuclear observables using standard perturbation theory. The matrix elements of the interaction hamiltonian between eigenstates of the noninteracting system, Fermi gas states in the case of uniform nuclear matter, turn out to be very large, or even divergent.

In the G -matrix approach the above problem is circumvented replacing the bare NN potential with the *well behaved* operator G , defined through the Bethe-Goldstone equation

$$\begin{aligned} \langle ij | G(E) | kl \rangle &= G_{ij,kl}(E) \\ &= v_{ij,kl} + \sum_{mn} v_{ij,mn} \frac{Q_{mn}}{E - \epsilon_m - \epsilon_n + i\eta} G_{mn,kl}(E), \end{aligned} \quad (5)$$

where $i \equiv (\mathbf{k}_i, s_i, t_i)$, \mathbf{k}_i , s_i and t_i being the momentum and the spin and isospin projections specifying the i -th single particle state. The Pauli operator Q_{mn} restrict the sum over intermediate states to those compatible with the exclusion principle, while the so-called starting energy E corresponds to the sum of the non-relativistic energies of the interacting nucleons.

The single-particle energy of a nucleon in the state i is given by

$$\epsilon_i = \frac{k_i^2}{2m} + Re[U_i], \quad (6)$$

where U_i describes the mean field felt by the nucleon due to its interactions with the other particles of the medium. In the so-called Brueckner-Hartree-Fock approximation, U_i is calculated in the ‘‘on-shell approximation’’ through a self-consistent process. The resulting expression is

$$U_i = \sum_{j \in \{F\}} \langle ij | G(E = \epsilon_i + \epsilon_j) | ij \rangle_a, \quad (7)$$

where the sum runs over all occupied states in the Fermi sea $\{F\}$ and the two-nucleon matrix elements are properly antisymmetrized. We note here that the so-called continuous prescription [17] has been adopted for the single-particle potential when solving the Bethe-Goldstone equation. As shown in Ref.[18], the contribution to the energy per particle from three-hole line diagrams is minimized by this prescription.

Once a self-consistent solution of the G -matrix is achieved, the energy per particle at the two-hole line level takes the form

$$\frac{E}{A} = \frac{3}{5} \frac{k_F^2}{2m} + \frac{1}{2} \sum_{i,j \in \{F\}} \langle ij | G(E = \epsilon_i + \epsilon_j) | ij \rangle_a, \quad (8)$$

where k_F is the Fermi momentum, related to the density through the relation $\rho = \nu k_F^3 / 6\pi^2$, ν being the spin-isospin degeneracy of the momentum eigenstates ($\nu = 2$ and 4 for pure neutron matter and symmetric nuclear matter, respectively).

In the approach based on correlated wave functions one uses the bare potential, v , whose non perturbative effects are incorporated in the basis states, obtained from the Fermi gas states $|n_{FG}\rangle$ through the transformation

$$|n\rangle = F |n_{FG}\rangle. \quad (9)$$

The operator F , embodying the correlation structure induced by the NN interaction, is written in the form

$$F = \mathcal{S} \prod_{ij} f_{ij}, \quad (10)$$

where \mathcal{S} is the symmetrization operator accounting for the fact that, in general, $[f_{ij}, f_{ik}] \neq 0$. The two-body correlation functions f_{ij} , whose operator structure reflects the complexity of the NN potential, is written in

the form

$$f_{ij} = \sum_{n=1}^6 f^n(r_{ij}) O_{ij}^n, \quad (11)$$

with the O_{ij}^n given by Eq.(3).

Within the correlated basis functions (CBF) approach, at two-body cluster level one finds [9, 10]

$$\frac{E}{A} = \frac{3}{5} \frac{k_F^2}{2m} + \sum_{j>i} \langle ij | V_{\text{eff}} | ij \rangle_a, \quad (12)$$

where

$$V_{\text{eff}} = \sum_{i<j} f_{ij}^\dagger \left[-\frac{1}{m} (\nabla^2 f_{ij}) - \frac{2}{m} (\nabla f_{ij}) \cdot \nabla + v_{ij} f_{ij} \right], \quad (13)$$

and the derivatives act on the relative coordinates.

One would be tempted to exploit the analogies between Eqs.(8) and (12), to establish a direct link between G and V_{eff} . However, determining such a connection at operator level is not trivial. To see this, just consider that, while all matrix elements of G involve the bare interaction v only, the matrix elements of V_{eff} also include purely kinetic contributions, not containing v , which arise from the derivatives of the correlation functions. In addition, unlike V_{eff} , G exhibits an explicit energy dependence.

The CBF effective interaction, being defined through its ground state expectation value, is somewhat limited in scope, with respect to the G -matrix effective interaction. However, a systematic comparison between the two formalisms can be carried out at the level of matrix elements. In this work we will focus on the matrix elements of the effective interactions in momentum space relevant to the calculation of the NN scattering rate in pure neutron matter, whose knowledge is required to obtain the transport coefficients within the Landau-Abrikosov-Khalatnikov formalism.

We have used the truncated version of the Argonne v_{18} potential referred to as v'_6 [19], whose definition only involves the static contributions, i.e. those corresponding to $n \leq 6$, in Eq.(3). The CBF effective interaction derived from this potential has been also used to obtain weak response of nuclear matter at moderate momentum transfer [9, 20].

For the sake of simplicity, in this work we have neglected the contribution of the three nucleon potential appearing in Eq.(1).

III. NN SCATTERING IN THE NUCLEAR MEDIUM

A. Kinematics

Consider the process in which two nucleons carrying momenta \mathbf{k}_1 and \mathbf{k}_2 scatter to final states of momenta

\mathbf{k}'_1 and \mathbf{k}'_2 . The total energy of the initial state

$$E = \frac{\mathbf{k}_1^2}{2m} + \frac{\mathbf{k}_2^2}{2m} \quad (14)$$

can be conveniently rewritten in terms of the center of mass and relative momenta, $\mathbf{K} = \mathbf{k}_1 + \mathbf{k}_2$ and $\mathbf{k} = (\mathbf{k}_1 - \mathbf{k}_2)/2$, as

$$E = \frac{\mathbf{K}^2}{2M} + \frac{\mathbf{k}^2}{2\mu} = \mathcal{E} + \mathcal{E}_{\text{rel}}, \quad (15)$$

with $M = 2m$ and $\mu = m/2$.

In the reference frame in which the center of mass of the system is at rest (CM frame) $E = E_{\text{CM}} = \mathcal{E}_{\text{rel}}$, while in the lab (L) frame, in which $\mathbf{k}_2 = 0$, $E = E_{\text{L}} = 2\mathcal{E}_{\text{rel}}$.

The analysis of the NN scattering rates relevant to the calculation of the transport coefficients is carried out in the frame in which the Fermi sphere is at rest, often referred to as Abrikosov-Khalatnikov (AK) frame. Moreover, in the low-temperature regime, in which the results of Ref.[3] are applicable, scattering processes can only involve nucleons with momenta close to the Fermi momentum. Therefore, one can set

$$|\mathbf{k}_1| = |\mathbf{k}_2| = |\mathbf{k}'_1| = |\mathbf{k}'_2| = k_F. \quad (16)$$

At energies below pion production threshold the scattering process is elastic, so that the requirement of energy conservation

$$\begin{aligned} (\mathbf{k}_1 + \mathbf{k}_2)^2 &= 2k_F^2(1 + \cos \theta) \\ &= (\mathbf{k}'_1 + \mathbf{k}'_2)^2 = 2k_F^2(1 + \cos \theta'), \end{aligned} \quad (17)$$

implies that the angle between the momenta of the two nucleons is the same before and after the collision. In general, however, the angle ϕ between the initial and final relative momenta, \mathbf{k} and $\mathbf{k}' = (\mathbf{k}'_1 - \mathbf{k}'_2)/2$, defined through

$$\cos \phi = \frac{(\mathbf{k} \cdot \mathbf{k}')}{|\mathbf{k}| |\mathbf{k}'|} \quad (18)$$

does not vanish. Hence, for any given Fermi momentum, i.e. for any given matter density, the scattering process in the AK frame is specified by the center of mass energy

$$\mathcal{E}_{\text{AK}} = \frac{k_F^2}{2m} (1 + \cos \theta), \quad (19)$$

and the two angles θ and ϕ .

As the NN scattering cross section is often evaluated in the CM frame, it is convenient to establish a relationship between kinematical variables in the CM and AK frames. Exploiting the frame invariance of the relative energy we easily obtain

$$E_{\text{CM}} = \frac{k_F^2}{2m} (1 - \cos \theta), \quad (20)$$

while the center of mass scattering angle θ_{CM} can be identified with ϕ , defined in Eq.(18).

B. Cross section

In both the G -matrix and CBF effective interaction approaches, the NN cross section in matter at density ρ , can be written in the form

$$\frac{d\sigma}{d\Omega_{\mathbf{k}'}} = \frac{m^{*2}}{16\pi^2} \sum_{SM M'} |\mathcal{M}_S^{MM'}(\theta, \phi)|^2, \quad (21)$$

where m^* is the nucleon effective mass, and the transition amplitude in the channel of total spin S and initial and final spin projections M and M' , $\mathcal{M}_S^{MM'}(\theta, \phi)$, involves the matrix elements of either G or V_{eff} between Fermi gas states.

Numerical calculations of the cross sections are carried out expanding $\mathcal{M}_S^{MM'}(\theta, \phi)$ in partial waves. In the case of pure neutron matter, in which the total isospin of the interacting pair is $T = 1$, the expansion only involves partial waves of even (odd) angular momentum in spin singlet (triplet) states.

The matrix elements of the CBF effective interaction can be written in the form

$$M_{\ell\ell'}^{S J}(k) = \frac{2}{\pi} \int r^2 dr j_\ell(kr) \langle \ell' S J | V_{\text{eff}} | \ell S J \rangle j_{\ell'}(kr). \quad (22)$$

In the above equation, ℓ and J denote orbital and total angular momentum, respectively, j_ℓ is the spherical Bessel function, $|\ell S J\rangle$ is the spin-angle state and r is the magnitude of the relative distance. Note that, due to the presence of the tensor operator of Eq.(4), the NN potential couples states of different orbital angular momentum. The above matrix elements are directly comparable with those obtained from the partial wave expansion of the G -matrix (see Eq.(5)).

In Fig. 1 we show the matrix element $M(^1S_0) = M_{00}^{00}$, evaluated at nuclear matter equilibrium density, $\rho_0 = 0.16 \text{ fm}^{-3}$ (top panel), and $2\rho_0$ (bottom panel), in the kinematical setup described in Section III A. The solid and dashed lines correspond to the matrix elements of the CBF and G -matrix effective interactions, respectively, while the dot-dash line has been obtained replacing V_{eff} with the bare v'_6 potential. Renormalization of the NN interaction, carried out either solving the Bethe-Goldstone equation or modifying the basis states, appears to have a strong impact on the matrix elements, which become more attractive with respect to the matrix elements of the bare interaction. On the other hand, CBF and G -matrix approaches yield rather similar results in the considered range of densities and momenta.

The matrix elements $M(^3P_2) = M_{11}^{12}$ are shown in Fig. 2. It appears that in this channel the results obtained using the CBF are closer to those corresponding to the bare interaction, while being appreciably different from the G -matrix results. Note, however, that the matrix elements corresponding to the 3P_2 channel are over one order of magnitude smaller than those corresponding to the 1S_0 channel.

It has to be pointed out that the density dependence of the matrix elements is rather mild. In the CBF approach

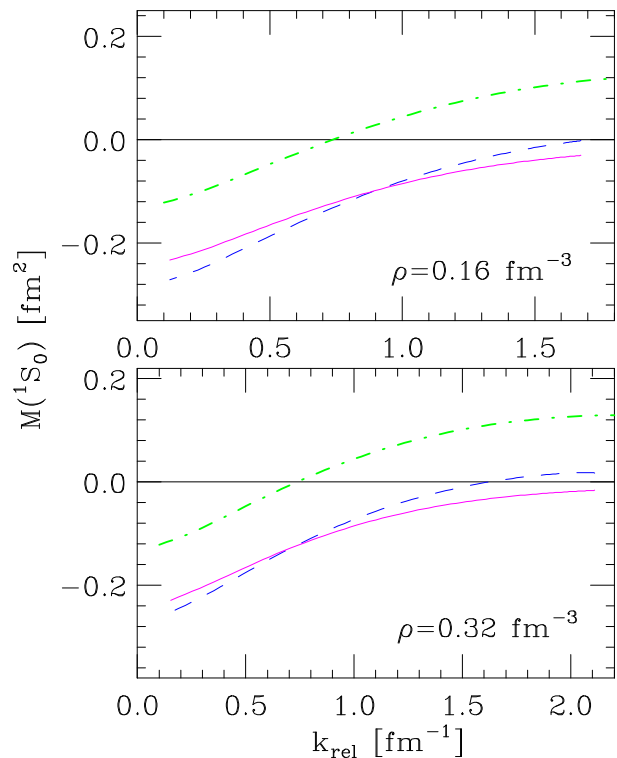


FIG. 1: (Color online) Top panel: $M(^1S_0)$ matrix element of the CBF (solid lines) and G -matrix (dashed lines) effective interactions (M_{00}^{00} of Eq.(22)) for neutron matter at nuclear matter equilibrium density, as a function of relative momentum. For comparison, the dot-dash line shows the result corresponding to the bare v'_6 potential. Bottom panel: same as the top panel, but for density $\rho = 2\rho_0$.

the density dependence arises from the two-body correlation functions, while in the G -matrix it comes through the presence of the Pauli operator and the single particle potentials appearing in the denominator of Eq.(5). In addition, one should also take into account the density dependence associated with the starting energy E , as the matrix elements reported in the Figs. 1 and 2 have been computed at twice the Fermi energy of the corresponding density.

The convergence of the partial wave expansion is illustrated in Fig. 3, showing the ratio

$$R_L = \frac{1}{\sigma_{\text{tot}}} \sum_{\ell=0}^L \sigma_{\text{tot}}^{\ell}, \quad (23)$$

as a function of CM energy (see Eq.(20)). In the above equation σ_{tot} is the total in-medium neutron-neutron cross section, while $\sigma_{\text{tot}}^{\ell}$ denotes the contribution of the ℓ -th partial wave. All cross sections have been evaluated in the kinematical set up relevant to the calculation of the transport coefficients, discussed in Section III A. The definition obviously implies that, as $L \rightarrow \infty$, $R_L \rightarrow 1$.

The results of Fig. 3 show that the total cross sections obtained including only the partial waves with $\ell = 0$

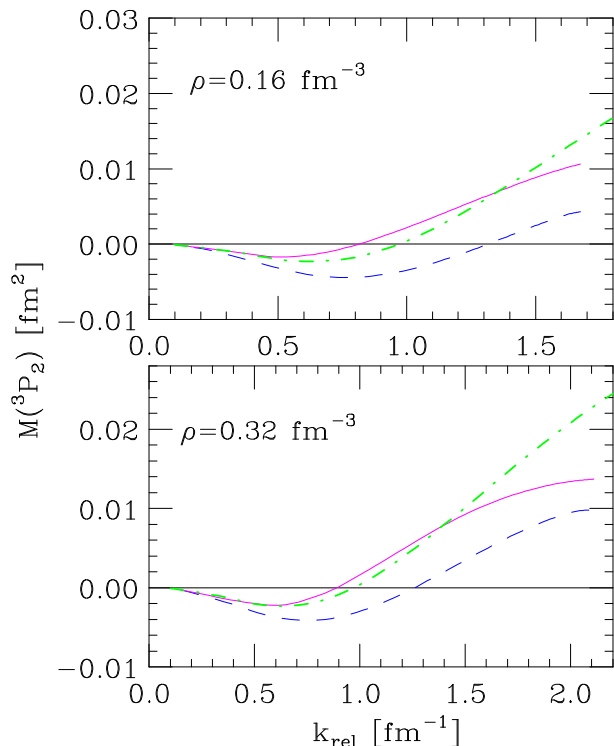


FIG. 2: (Color online) Same as in Fig. 1, but for the $M(^3P_2)$ matrix elements.

and 1, corresponding to the spin-singlet and spin-triplet states of lowest angular momentum, is within less than 5% of the fully converged result. Comparison between the top and bottom panels, corresponding to *CBF* and *G*-matrix effective interactions, also shows that the two approaches lead to a similar qualitative behavior, although the *G*-matrix R_0 exhibit a somewhat steeper energy dependence.

In Fig. 4 we compare the total neutron-neutron cross section at nuclear matter equilibrium density, computed in the kinematics of Section III A, as a function of E_{CM} . The difference between the cross sections obtained using the *CBF* (solid line) and *G*-matrix (dashed line) approaches does not exceed $\sim 20\%$ at $E_{\text{CM}} > 10$ MeV. On the other hand, the screening effect due to the presence of the nuclear medium, illustrated by the difference between the solid and dashed lines and the dot-dashed one, corresponding to the free-space cross section obtained from the *t*-matrix associated with the v'_6 potential, turns out to be large. At $E_{\text{CM}} > 100$ MeV, where the *CBF* and *G*-matrix results are very close to one another, the in medium cross section turns out to be quenched by a factor ~ 3 .

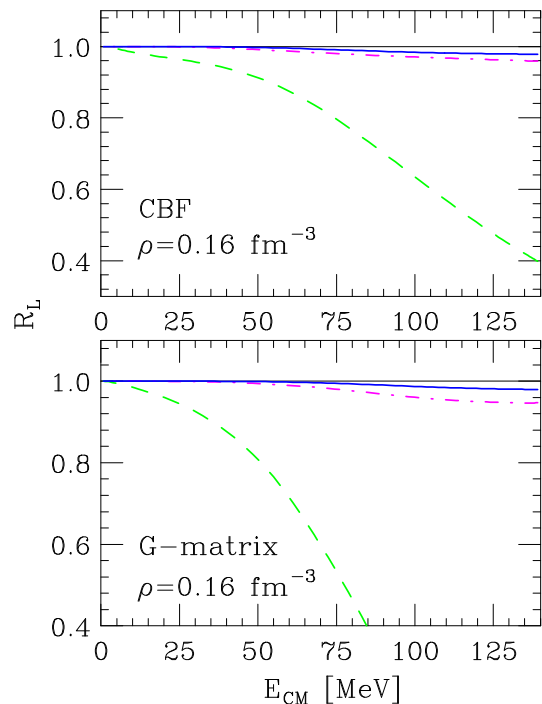


FIG. 3: (Color online) Energy dependence of the ratio R_L , defined by Eq.(23). The dashed, dot-dash and solid lines have been obtained including the contributions of states of angular momentum ℓ up to 0, 1 and 2. The top and bottom panels correspond to *CBF* and *G*-matrix effective interactions, respectively.

IV. TRANSPORT COEFFICIENTS

A. Abrikosov-Khalatnikov formalism

The theoretical description of transport properties of normal Fermi liquids is based on Landau theory [4]. Working within this framework and including the leading term in the low-temperature expansion, Abrikosov and Khalatnikov [3] obtained approximate expressions for the shear viscosity and the thermal conductivity. Let us consider viscosity, as an example. The AK result reads

$$\eta_{\text{AK}} = \frac{1}{5} \rho m^* v_F^2 \tau \frac{2}{\pi^2 (1 - \lambda_\eta)}, \quad (24)$$

where $v_F = k_F/m^*$ is the Fermi velocity and m^* and τ denote the quasiparticle effective mass and lifetime, respectively. The latter can be written in terms of the angle-averaged scattering probability, $\langle \mathcal{W} \rangle$, with (see Eq.(21))

$$\mathcal{W}(\theta, \phi) = \sum_{SMM'} |\mathcal{M}_S^{MM'}(\theta, \phi)|^2, \quad (25)$$

according to

$$\tau T^2 = \frac{8\pi^4}{m^{*3}} \frac{1}{\langle \mathcal{W} \rangle}, \quad (26)$$

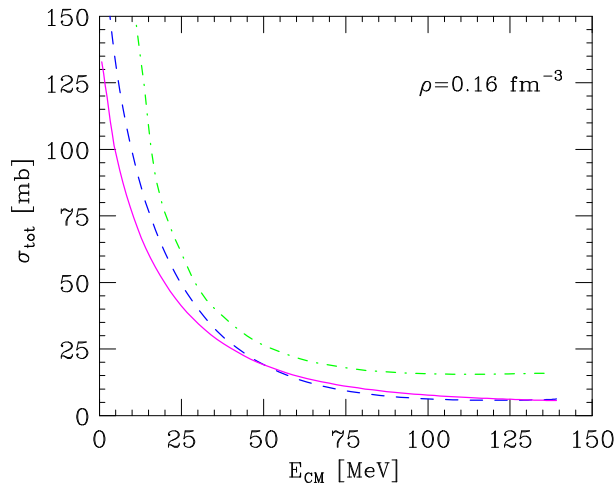


FIG. 4: (Color online) Total in-medium neutron-neutron cross section in neutron matter, computed at nuclear matter equilibrium density as a function of energy in the center of mass frame. The solid and dashed lines have been obtained using the CBF and G -matrix effective interactions, respectively, in the kinematical setup discussed in Section III A. For comparison, the dot-dash line shows the free-space cross section, obtained from the t -matrix associated with the v'_6 potential.

where T is the temperature and

$$\langle \mathcal{W} \rangle = \int \frac{d\Omega}{2\pi} \frac{\mathcal{W}(\theta, \phi)}{\cos(\theta/2)}. \quad (27)$$

Note that, as pointed out in Section III A, the scattering process involves quasiparticles on the Fermi surface. As a consequence, for any given density ρ , \mathcal{W} depends only on the angular variables θ and ϕ . Finally, the quantity λ_η appearing in Eq.(24) is defined as

$$\lambda_\eta = \frac{\langle \mathcal{W}[1 - 3 \sin^4(\theta/2) \sin^2 \phi] \rangle}{\langle \mathcal{W} \rangle}. \quad (28)$$

The exact solution of the equation derived in Ref. [3], obtained by Brooker and Sykes [21], reads

$$\eta = \eta_{AK} \frac{1 - \lambda_\eta}{4} \times \sum_{k=0}^{\infty} \frac{4k + 3}{(k+1)(2k+1)[(k+1)(2k+1) - \lambda_\eta]}, \quad (29)$$

the size of the correction with respect to the result of Eq.(24) being $0.750 < (\eta/\eta_{AK}) < 0.925$.

The expression of the thermal conductivity, κ , is obtained following the same procedure, the only difference being that in this case the leading term in the low energy expansion is linear, rather than quadratic, in the inverse temperature T^{-1} . The resulting expression is

$$\kappa = \kappa_{AK} \frac{3 - \lambda_\kappa}{4} \times \sum_{k=0}^{\infty} \frac{4k + 5}{(k+1)(2k+3)[(k+1)(2k+3) - \lambda_\kappa]}, \quad (30)$$

where

$$\kappa_{AK} = \frac{1}{T} \frac{8}{3} \frac{k_F^3}{m^{*4}} \frac{2\pi^2}{\langle \mathcal{W} \rangle (3 - \lambda_\kappa)} \quad (31)$$

and

$$\lambda_\kappa = \frac{\langle \mathcal{W}(1 + 2 \cos \theta) \rangle}{\langle \mathcal{W} \rangle}. \quad (32)$$

In this case the correction to the AK result turns out to be larger. From Eq.(32) it follows that $-1 < \lambda_\kappa < 3$, implying in turn (see Eq.(30)) $0.417 < (\kappa/\kappa_{AK}) < 0.561$.

B. Results

Figures 5 and 6 show the T -independent quantities ηT^2 and κT , respectively, as a function of density. The calculations have been carried out using the formalism described in the previous Section and the scattering probabilities $\mathcal{W}(\theta, \phi)$ obtained from both the G -matrix and CBF effective interactions, which have been computed at zero temperature. For comparison, in Fig. 5 we also display, by the dot-dash line, the results obtained from the free-space scattering probability, computed using the t -matrix associated with the bare v'_6 potential.

As the ratios m^*/m resulting from the two approaches, CBF and G -matrix, turn out to be rather close to one another (the difference never exceeds few percent in the density range shown in Figs. 5 and 6) all calculations have been carried out using the CBF effective masses.

Figure 5 clearly indicates that medium modifications of the NN scattering cross sections play a critical role, leading to a dramatic enhancement of the viscosity. A similar effect is observed in the case of thermal conductivity [22].

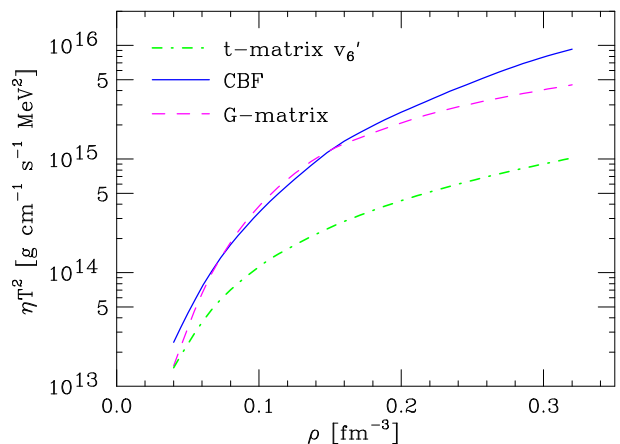


FIG. 5: (Color online) Density dependence of the T -independent quantity ηT^2 in pure neutron matter. The solid and dashed lines correspond to the CBF and G -matrix effective interactions, respectively, while the dot-dash line shows the results obtained from the t -matrix associated with the v'_6 potential.

Comparison between Fig. 5 and Fig. 6 shows that, while the density dependence of the thermal conductivity resulting from the two approaches looks remarkably similar, in the case of viscosity sizable discrepancies occur at densities larger than nuclear matter equilibrium density.

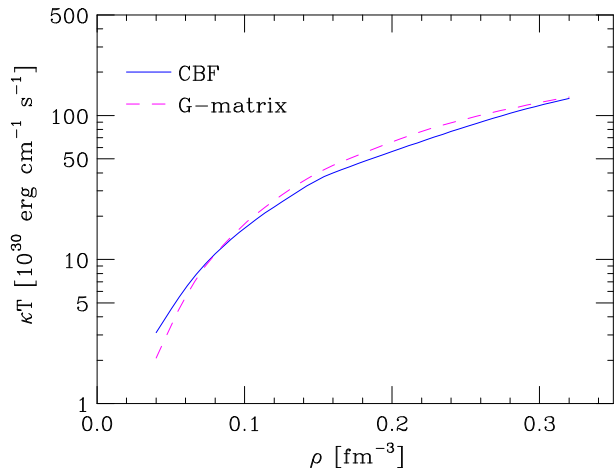


FIG. 6: (Color online) Density dependence of the T -independent quantity κT in pure neutron matter. The solid and dashed lines have been obtained using the CBF and G -matrix effective interactions, respectively.

This feature can be easily explained considering the different angular dependence of the integrands in Eqs.(28) and (32), which determine the functions λ_η and λ_κ , respectively. In the case of λ_κ , $\mathcal{W}(\theta, \phi)$ is weighted with a function that only depends on θ . As a consequence, the result only depends on the ϕ -integrated scattering probability, which is trivially related to the *total* cross section (see Eq.(21)) at energy E_{CM} given by Eq.(20). Hence, the similar behavior exhibited by the two curves of Fig. 6 merely reflects the fact that the total cross sections obtained from the G -matrix and CBF approaches turn out to be close to one another (see Fig. 4). On the other hand, in the right hand side of Eq.(28) the scattering probability is weighted with a factor that emphasizes the differences in the ϕ dependence of the CBF and G -matrix $\mathcal{W}(\theta, \phi)$.

We have verified that the large discrepancy between the solid and dashed curves of Fig. 5 at high density is in fact ascribable to λ_η . The λ_η -independent quantities $\eta_{AK}(1 - \lambda_\eta)/4$ obtained from the CBF and G -matrix approaches turn out to be within less than 5 % of one another at $\rho = 0.32 \text{ fm}^{-3}$. On the other hand, removal of the λ_κ dependence in κ_{AK} does not produce any significant effects.

V. CONCLUSIONS

Many body theory provides a fully consistent framework, suited to construct effective interactions starting

from highly realistic models of nuclear dynamics. In this work, we have employed the effective interactions resulting from the G -matrix and CBF approaches to compute the in-medium NN cross sections, which are needed to obtain the transport coefficient within the Landau-Abrikosov-Khalatnikov formalism.

The calculations have been carried out using the truncated v'_6 form of the NN potential of Ref. [11]. The effects of three- and many-body forces, though being known to be sizable at large density, have not been taken into account. The results of Ref. [10] show that many-body forces give rise to a change of the shear viscosity of less than 10 % at $\rho \lesssim 0.32 \text{ fm}^{-3}$. Hence, their inclusion is not likely to significantly affect the main conclusions of our work.

The approach based on effective interactions allows one to consistently take into account screening effects arising from short range NN correlations, that lead to a large decrease of the scattering cross section. As a consequence, the shear viscosity and thermal conductivity obtained from the effective interactions turn out to be much larger than the corresponding quantities computed using the bare NN potential.

Our work, showing that the results of the G -matrix and CBF schemes are in reasonable agreement with one another, suggests that as long as the effective interaction is based on a *realistic* NN potential, strongly constrained by the large data set of NN scattering phase shifts, the model dependence associated with the many body approach employed is not critical.

On the other hand, it has to be pointed out that Skyrme effective interactions (for a recent and comprehensive discussion the application of the Skyrme approach to nuclear matter and neutron stars see Ref.[23]), mainly constructed by fitting bulk properties of nuclear matter, predict in-medium NN cross sections whose behavior is significantly different from the one predicted by the G -matrix and CBF effective interactions. As a result, the values of the viscosity and thermal conductivity coefficients computed using Skyrme effective interactions turn out to be much lower than those shown in Figs. 5 and 6. For example, using the SLya effective interaction, adjusted to reproduce the the microscopically derived EOS of neutron and nuclear matter [24], one finds at nuclear matter equilibrium density $\eta T^2 \sim 6 \times 10^{13} \text{ g cm}^{-1} \text{ s}^{-1} \text{ MeV}^2$ and $\kappa T \sim 4 \times 10^{30} \text{ erg cm}^{-1} \text{ s}^{-1}$, to be compared to $\sim 1.4 \times 10^{15} \text{ g cm}^{-1} \text{ s}^{-1} \text{ MeV}^2$ and $\kappa T \sim 4 \times 10^{31} \text{ erg cm}^{-1} \text{ s}^{-1}$ obtained from the G -matrix and CBF formalisms. While the Skyrme approach has proved to be very useful in many contexts, these results suggest that the determination of the transport properties of nuclear matter requires effective interactions providing a quantitative account of the observed NN scattering data in the limit of vanishing density.

Acknowledgments

This work was partially supported by FEDER/FCT (project CERN/FP/83505/2008), Consolider-Ingenio 2010 (programa CPAN CSD2007-00042 and grant

FIS2008-01661), MEC/FEDER (project 2009SGR-1289) and the European Science Foundation research networking program COMPSTAR. MV gratefully acknowledges the hospitality of the Departament d'Estructura i Constituents de la Matèria, Barcelona.

-
- [1] N. Anderson and K.D. Kokkotas, *Int. J. Mod. Phys.* **10**, 381 (2001).
 - [2] D.G. Yakovlev, A.D. Kaminker, O.Y. Gnedin and P. Haensel, *Phys. Rep.* **66**, 1 (2001).
 - [3] A.A. Abrikosov and I.M. Khalatnikov, *Soviet Phys. JETP* **5**, 887 (1957); *Rep. Prog. Phys.* **22**, 329 (1959).
 - [4] G. Baym and C. Pethick, *Landau Fermi-Liquid Theory* (John Wiley & Sons, New York, 1991).
 - [5] E. Flowers and N. Itoh, *Astrophys. J.* **206**, 218 (1976).
 - [6] E. Flowers and N. Itoh, *Astrophys. J.* **230**, 847 (1979).
 - [7] D.A. Baiko and P. Haensel, *Acta Phys. Pol.* **30**, 1097 (1999).
 - [8] J. Wambach, T.L. Aisworth and D. Pines, *Nucl. Phys.* **555**, 128 (1993).
 - [9] S. Cowell and V.R. Pandharipande, *Phys. Rev. C* **73**, 025801 (2006).
 - [10] O. Benhar and M. Valli, *Phys. Rev. Lett.*, **99**, 232501 (2007).
 - [11] R.B. Wiringa, V.G.J. Stocks and R. Schiavilla, *Phys. Rev. C* **51**, 38 (1995).
 - [12] B.S. Pudliner, V.R. Pandharipande, J. Carlson and R.B. Wiringa, *Phys. Rev. Lett.* **74**, 4369 (1995).
 - [13] S.C. Pieper and R.B. Wiringa, *Ann. Rev. Nucl. Part. Sci.* **51**, 53 (2001).
 - [14] K.S. A. Sarsa, S. Fantoni and F. Pederiva, *Phys. Rev. C* **68**, 024308 (2003).
 - [15] A. Akmal, V.R. Pandharipande and D. Ravenhall, *Phys. Rev. C* **58**, 1804 (1998).
 - [16] H. Mütter and A. Polls, *Prog. Part. Nucl. Phys.* **45**, 243 (2000)
 - [17] M. Baldo in *Nuclear Methods and the nuclear equation of state*, edited by M. Baldo, International Review of Nuclear Physics, Vol. 8, World Scientific, Singapore, 1999.
 - [18] H.Q. Song, M. Baldo, G. Giansiracusa and U. Lombardo, *Phys. Rev. Lett.* **81**, 1584 (1998).
 - [19] B.S. Pudliner, V.R. Pandharipande, J. Carlson, S.C. Pieper and R.B. Wiringa, *Phys. Rev. C* **56**, 1720 (1997).
 - [20] O. Benhar and N. Farina, *Phys. Lett.* **B680**, 305 (2009).
 - [21] G.A. Brooker and J. Sykes, *Phys. Rev. Lett.* **21**, 279 (1968).
 - [22] O. Benhar, N. Farina, S. Fiorilla and M. Valli, *AIP Conf.Proc.* **1056**, 248 (2008).
 - [23] J.R. Stone, J.C. Miller, R. Koncewicz, P.D. Stevenson and M.R. Strayer, *Phys. Rev. C* **68**, 034324 (2003).
 - [24] E. Chabanat, P. Bonche, P. Haensel, J. Meyer and R. Schaeffer, *Nucl. Phys.* **A627**, 710 (1997).